

**ISCI, Volume 10**

**Supplemental Information**

**Surface-Enhanced Raman Spectroscopy  
on Amorphous Semiconducting  
Rhodium Sulfide Microbowl Substrates**

**Anran Li, Jie Lin, Zhongning Huang, Xiaotian Wang, and Lin Guo**

## Supplemental Information

### 1. Supplemental Data Items

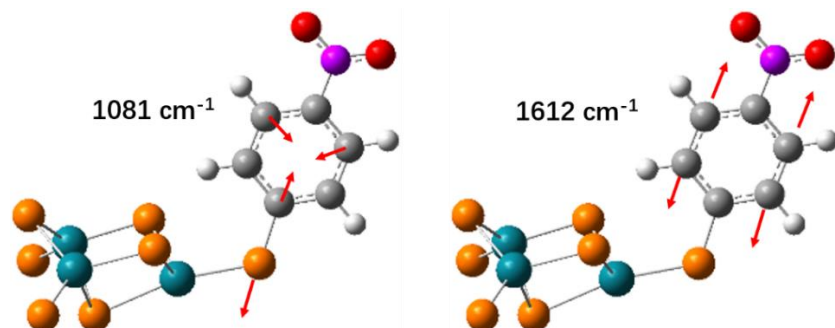


**Figure S1.** Calculation of the normal modes for 4NBT adsorbed on Rh<sub>3</sub>S<sub>6</sub> cluster, related to Figure 1. Calculation of the  $\sim 1081\text{ cm}^{-1}$  and  $\sim 1612\text{ cm}^{-1}$  modes, corresponding to the ring-breathing mode coupled to the C-S stretch mode and the C=C stretching mode, respectively.

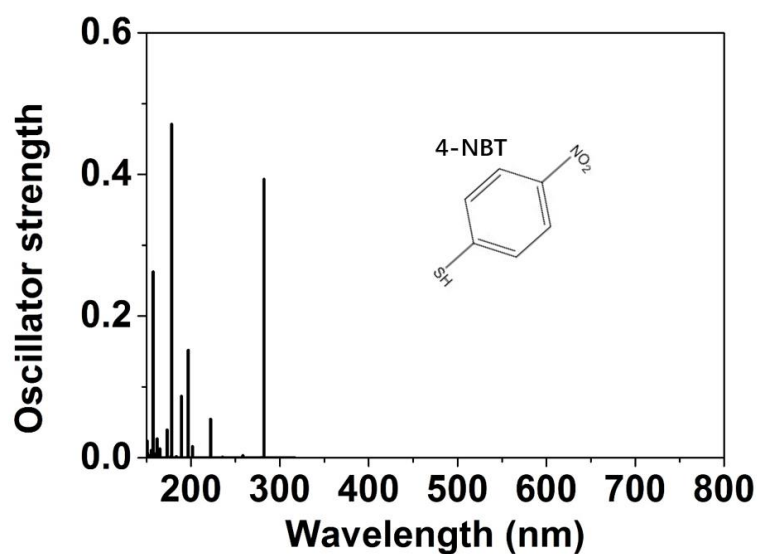


**Figure S2.** TDDFT calculation of a 4NBT molecule, related to Figure 2. Calculated vertical transition energies and oscillator strength of a 4NBT molecule.

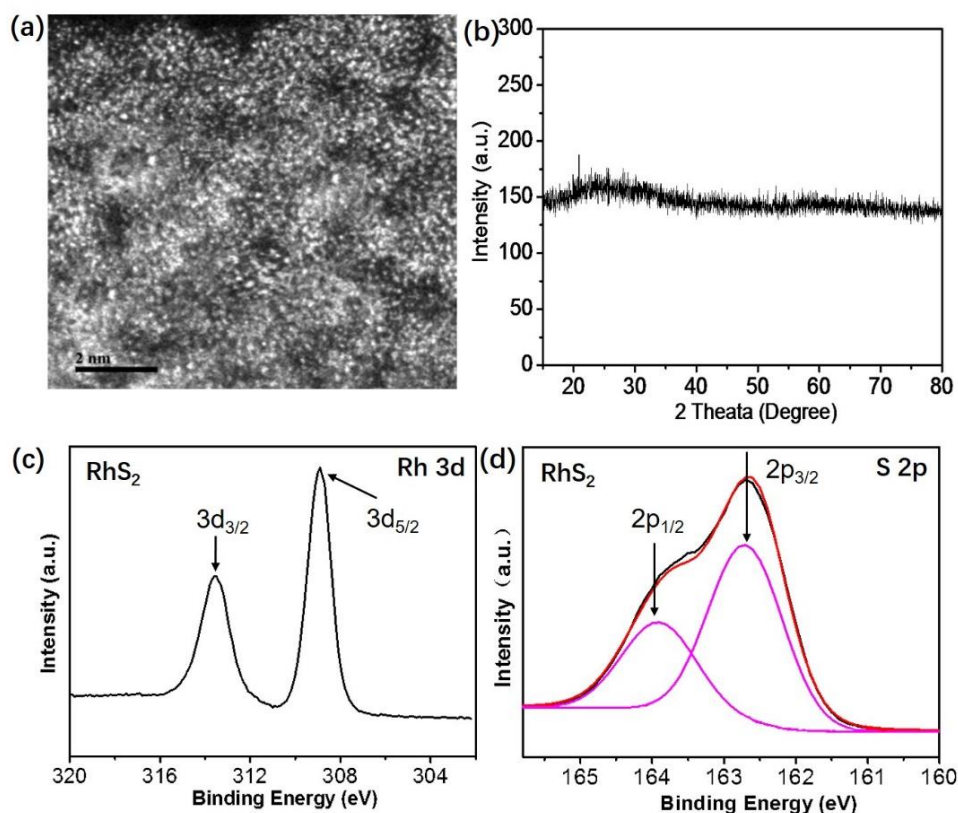


**Figure S3. Characterization of the synthesized amorphous rhodium sulfide microbowls, related to Figure 3.** (a) The Spherical Aberration Corrected Transmission Electron Microscope (ACTEM) image of the amorphous rhodium sulfide microbowls. (b) X-ray Diffraction (XRD) of the amorphous rhodium sulfide microbowls. (c and d) X-ray photoelectron spectroscopy (XPS) spectra of the amorphous rhodium sulfide microbowls.

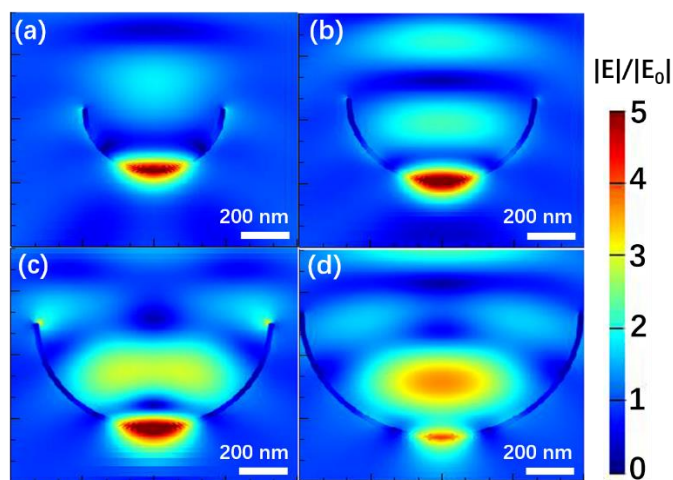


**Figure S4. FDTD calculation of the amorphous rhodium sulfide microbowls, related to Figure 3.** Calculated electric field distributions ( $|E|/|E_0|$ ) for amorphous rhodium sulfide microbowls with various diameters. (a) 0.6  $\mu\text{m}$  (b) 0.8  $\mu\text{m}$  (c) 1  $\mu\text{m}$  and (d) 1.2  $\mu\text{m}$ .

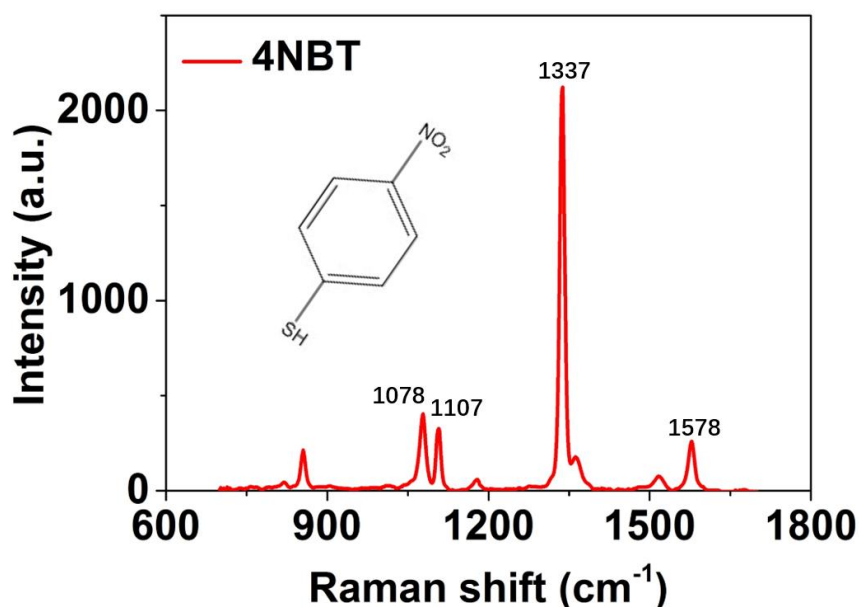


**Figure S5.** Normal Raman spectrum of the 4NBT at the concentration of  $1 \times 10^{-2}$  mol/L at 633 nm, related to Figure 3. The main peaks at  $1578 \text{ cm}^{-1}$ ,  $1337 \text{ cm}^{-1}$ , and  $\sim 1100 \text{ cm}^{-1}$  were attributed to the C=C stretching mode of the benzene ring, the symmetric stretching vibration of the nitro group ( $\text{NO}_2$ ), and the ring-breathing mode coupled to the C-S stretch mode, respectively (Shin et al., 2014).

**Table S1.** Enhancement factor (EF) and limit of detection (LOD) of various semiconductors in previous reports (Cong et al., 2015; Jiang et al., 2013; Liu et al., 2014; Qi et al., 2014; Wang et al., 2017; Wang et al., 2011; Zheng et al., 2017). Results in this work is in bold. **Related to Figure 4.**

Material	Analyte	EF	LOD (M)	Laser (nm)	Reference
<b>amorphous rhodium sulfide</b>	<b>R6G</b>	<b><math>1 \times 10^5</math></b>	<b><math>10^{-7}</math></b>	<b>647</b>	<b>this work</b>
amorphous ZnO	4-MBA	$6.62 \times 10^5$	---	633	Wang et al., 2017
urchin-like $\text{W}_{18}\text{O}_{49}$	R6G	$3.4 \times 10^5$	$10^{-7}$	522	Cong et al., 2015
ZnO nanosheet	4-MBA	---	$10^{-6}$	514.5	Liu et al., 2014
$\text{TiO}_2$ microarray	MB	$2 \times 10^4$	$6 \times 10^{-6}$	532	Qi et al., 2014
H-Si/H-Ge	R6G/N719	8-28	$10^{-6}$	532	Wang et al., 2011
$\text{Cu}_2\text{O}$ nanosphere	4-MBA	$10^5$	$10^{-3}$	488	Jiang et al., 2013
$\text{MoS}_2$	R6G	$9 \times 10^3$	---	532.8	Zheng et al., 2017
partially oxidized $\text{MoS}_2$ (optimum)	R6G	$1.4 \times 10^5$	$10^{-7}$	532.8	Zheng et al., 2017
$\text{WS}_2$	R6G	$2.5 \times 10^4$	---	532.8	Zheng et al., 2017

## 2. Transparent Methods

### 2.1 Computational Details

**First-principles calculations:** The density functional theory (DFT) and time-dependent density functional theory (TDDFT) calculations are employed to investigate the chemical enhancement mechanism of amorphous rhodium sulfide nanomaterial in surface-enhanced Raman scattering (SERS), including the geometry optimizations, ground-state properties, static Raman spectra, and vertical electronic transitions. All the calculations are implemented with the Gaussian 09 package (Frisch et al., 2010). A rhodium sulfide cluster ( $\text{Rh}_3\text{S}_6$ ) and a rhodium oxide cluster ( $\text{Rh}_3\text{O}_6$ ) are built based on the pre-demonstrated model of transition metal sulfide clusters (Cakır and Gülseren, 2012; Gemming et al., 2010; Guo et al., 2016; Mayhall et al., 2011). The Becke's three-parameter hybrid exchange functional and Lee,

Yang, and Parr's (B3LYP) exchange functional combined with the mixed basis sets are adopted for the structure optimization, and the calculation of the Raman spectra, the charge distribution, and the molecular orbital (Becke, 1993; Lee et al., 1988; Miehllich et al., 1989). The basis set for C, H, O, N, S atoms is 6-311+G (d,p), which includes the polarization function and the diffuse function. For Rh atom, the Lan12dz(Hay and Wadt, 1985) basis set is used to describe its valence electrons and internal shells. The B3LYP/6-311+G(d,p) level and B3LYP/Lan12dz level have been shown to be adequate describing the interaction of organic molecule and the transition metal sulfide cluster before. The TDDFT with the CAM-B3LYP functional is used to calculate the oscillator strength, which has been demonstrated to give a good accuracy in calculating the excited state energies (Mohammadpour and Jamshidi, 2016). In this study, all models are firstly fully optimized without imaginary frequency, guaranteeing that all the structures are in stable states. The calculated Raman spectra are broadened using a Lorentzian function with the full width at half maximum (FWHM) of 10  $\text{cm}^{-1}$ . The calculated absorption spectra are broadened using a Gaussian function with the FWHM of 0.6 eV.

**Finite-difference time-domain simulations:** The electric field distributions ( $|E|/|E_0|$ ) of amorphous rhodium sulfide microbowls and amorphous rhodium sulfide film are calculated using the 3D finite-difference time-domain (FDTD) method (Taflove and Hagness, 2005). For all simulations, a total-field scattered-field plane wave source is used to estimate the interaction between propagating plane waves and rhodium sulfide structures. Vacuum is taken as the external medium. The refractive index of amorphous rhodium sulfide is set at 4. The diameter and the wall thickness of the microbowl is 1  $\mu\text{m}$  and 20 nm, respectively. The thickness of the rhodium sulfide film is 20 nm. To get accurate results, all structures are enclosed by an override mesh region with 2 nm mesh size. The incident wavelength is 633 nm. All the calculations are performed using the Lumerical Solutions (FDTD solutions 8.6, Lumerical solutions, Inc., Vancouver, Canada).

## 2.2 Experimental Procedures

**Reagents:** rhodium(III) chloride hydrate ( $\text{RhCl}_3 \cdot 3\text{H}_2\text{O}$ ) is purchased from Alfa Aesar. Dimethyl sulfoxide (DMSO) is purchased from J&K Chemicals. The 98% concentrated sulphuric acid ( $\text{H}_2\text{SO}_4$ ) is purchased from Beijing Chemical Works. The 30% hydrogen peroxide ( $\text{H}_2\text{O}_2$ ) is purchased from Xilong Chemical Co., Ltd. All chemical reagents used in this experiment are analytical grade and used without further purification.

**Preparation of the amorphous rhodium sulfide microbowls:** The amorphous rhodium sulfide microbowls are synthesized via a hydrothermal method. In a typical synthesis, 1 mL 10 mg/mL rhodium(III) chloride hydrate is mixed with 30 mL dimethyl sulfoxide in a 100 mL flask at room temperature. The mixture is transferred into a water-bath which is kept at 20  $^\circ\text{C}$  for 10 min. Then, 3.4 mL 30%  $\text{H}_2\text{O}_2$  is added into the flask. After being stirred for 30 min, 4.5 mL 2 mol/L  $\text{H}_2\text{SO}_4$  is poured into the above solution, and the mixture is continuously maintained at 20  $^\circ\text{C}$  for 60 min afterwards. Subsequently, the flask is heated to 140  $^\circ\text{C}$  with oil-bath for 100 min under the magnetic stirring. After that, the mixture is centrifuged at 8000 rpm for 5 min and washed with ethanol for three times. Finally, the bowl-like rhodium sulfide nanomaterials in yellow color are obtained.

**Characterization:** The morphology and size of three-dimensional rhodium sulfide microbowls are characterized by scanning electron microscopy (SEM, 10kV, Quanta 250 FEG, FEI) and transmission electron microscopy (TEM, 200kV, JEM2100, JEOL). XRD patterns was performed by LabX XRD-6000.

**SERS measurements:** 4-nitro benzene thiol (4NBT) and rhodamine 6G (R6G) molecules are chosen as Raman target molecules. 50  $\mu\text{L}$  amorphous rhodium sulfide ethanol suspension is mixed with the 4NBT and R6G molecules dispersed in ethanol solution with different concentrations, respectively. The mixtures are placed for 5 hours and then 5  $\mu\text{L}$  of the mixed solution is dropped onto a clean Si substrate. The Si substrate is thoroughly rinsed for several times using the absolute ethanol to remove the free unadsorbed probe molecules. The Si samples are then subjected to Raman characterization. For all SERS measurements, 100  $\times$  objective, 0.8 mW power, and 10 s acquisition time are used to acquire the SERS spectra with 514 nm, 633 nm, 647 nm, and 785 nm excitation wavelengths. In addition, for each measurement, twenty SERS spectra from different randomly chosen positions are collected and then averaged for the final analysis.

## 2.3 Calculation of the SERS enhancement factor

The enhancement factor (EF) of the amorphous rhodium sulfide microbowls in SERS is calculated based on the equation  $EF = (I_{SERS}/N_{ads})/(I_{bulk}/N_{bulk})$ , where  $I_{SERS}$  and  $I_{bulk}$  are the SERS intensity of particular peak of the probe molecule and the normal Raman intensity of the probe molecule;  $N_{ads}$  and  $N_{bulk}$  are the number of the

molecules adsorbed on the SERS substrate and the number of molecules in normal Raman measurement.

For 4NBT molecules, the intensity of the C=C stretching mode ( $\sim 1576 \text{ cm}^{-1}$ ) is used to calculate the EF. In the experiment, 5  $\mu\text{L}$  4NBT ethanol solution with the concentration of  $1 \times 10^{-2} \text{ mol/L}$  is dried onto the Si wafer ( $0.3 \times 0.3 \text{ cm}^2$ ). The diameter of the laser spot is  $d = 1.22 \lambda/N_A$ , where  $\lambda$  is incident wavelength of 633 nm,  $N_A$  is the numerical aperture of the objective lens with the value of 0.5. Therefore, the laser spot size ( $\pi (d/2)^2$ ) is  $\sim 1.87 \mu\text{m}^2$ . Then,  $N_{bulk}$  is estimated to be:

$$N_{bulk} = 5 \mu\text{L} \times 1 \times 10^{-2} \text{ mol/L} \times 6.02 \times 10^{23} \text{ mol}^{-1} \times 1.87 \mu\text{m}^2 / 0.09 \text{ cm}^2 = 6.25 \times 10^9.$$

For determining the  $N_{ads}$ , we assume that the 4NBT molecules are adsorbed on the rhodium sulfide as a monolayer with the molecular footprint of  $\sim 0.7 \text{ nm}^2$  (Wang and Rothberg, 2005). Therefore,  $N_{ads}$  is estimated to be  $2.24 \times 10^6$  considering the laser spot size and the microbowl size (approximately one microbowl within the laser spot). In addition, according to Figure 3(g) and Figure S5,  $I_{SERS} = 3374$ , and  $I_{bulk} = 277$ . Therefore, the EF for 4NBT molecules adsorbed on the amorphous rhodium sulfide microbowls is calculated to be  $\sim 3 \times 10^4$ .

For R6G molecules, the intensity of the band centered at  $\sim 616 \text{ cm}^{-1}$  is used to calculate the EF of R6G adsorbed on the amorphous rhodium sulfide microbowls. 5  $\mu\text{L}$  R6G ethanol solution with the concentration of  $1 \times 10^{-2} \text{ mol/L}$  is dried onto the Si wafer ( $0.3 \times 0.3 \text{ cm}^2$ ) for normal Raman measurement. The diameter of the laser spot is  $d = 1.22 \lambda/N_A$ , where  $\lambda$  is incident wavelength of 647 nm,  $N_A$  is the numerical aperture of the objective lens with the value of 0.5. Therefore, the laser spot size ( $\pi (d/2)^2$ ) is  $\sim 1.96 \mu\text{m}^2$ . Then,  $N_{bulk}$  is estimated to be:

$$N_{bulk} = 5 \mu\text{L} \times 1.0 \times 10^{-2} \text{ mol/L} \times 6.02 \times 10^{23} \text{ mol}^{-1} \times 1.96 \mu\text{m}^2 / 0.09 \text{ cm}^2 = 6.56 \times 10^9.$$

According to Figure 4,  $I_{SERS}$  and  $I_{bulk}$  are determined to be 11730 and 613, respectively. In addition,  $N_{ads}$  is estimated to be  $1.25 \times 10^6$  by assuming the R6G molecules are adsorbed on the rhodium sulfide as a monolayer with the molecular footprint of  $1.2 \text{ nm}^2$  (the density of  $\sim 0.138 \text{ nM/cm}^2$ ) (Anderson and Bard, 1995). Therefore, the EF of R6G molecules adsorbed on the amorphous rhodium sulfide microbowls is estimated to be  $\sim 1 \times 10^5$ .

### 3. Supplemental References

Anderson, C., and Bard, A.J. (1995). An Improved Photocatalyst of  $\text{TiO}_2/\text{SiO}_2$  Prepared by a Sol-Gel Synthesis. *J. Phys. Chem.* 99, 9882-9885.

Becke, A.D. (1993). Density-functional thermochemistry. III. The role of exact exchange. *J. Chem. Phys.* 98, 5648-5652.

Hay, P.J., and Wadt, W.R. (1985). Ab initio effective core potentials for molecular calculations. Potentials for K to Au including the outermost core orbitals. *J. Chem. Phys.* 82, 299-310.

Lee, C., Yang, W., and Parr, R.G. (1988). Development of the Colle-Salvetti correlation-energy formula into a functional of the electron density. *Phys. Rev. B: Condens. Matter* 37, 785-789.

Miehlich, B., Savin, A., Stoll, H., and Preuss, H. (1989). Results obtained with the correlation energy density functionals of becke and Lee, Yang and Parr. *Chem. Phys. Lett.* 157, 200-206.

Mohammadpour, M., and Jamshidi, Z. (2016). Comparative assessment of density functional methods for evaluating essential parameters to simulate SERS spectra within the excited state energy gradient approximation. *J. Chem. Phys.* 144, 194302.

Qi, D., Lu, L., Wang, L., and Zhang, J. (2014). Improved SERS sensitivity on plasmon-free  $\text{TiO}_2$  photonic microarray by enhancing light-matter coupling. *J. Am. Chem. Soc.* 136, 9886-9889.

Taflove, A., and Hagness, S.C. (2005). Computational electrodynamics : the finite-difference time-domain method (Boston : Artech House, c2005. 3rd ed.).

Wang, Z., and Rothberg, L.J. (2005). Origins of Blinking in Single-Molecule Raman Spectroscopy. *J. Phys. Chem. B* *109*, 3387-3391.